

ManiFeel: Benchmarking and Understanding Visuotactile Manipulation Policy Learning

Quan Khanh Luu*, Pokuang Zhou*, Zhengtong Xu*, Zhiyuan Zhang,

Qiang Qiu, Yu She

* equal contribution
Purdue University

Abstract: Supervised visuomotor policies have shown strong performance in robotic manipulation but often struggle in tasks with limited visual input, such as operations in confined spaces, dimly lit environments, or scenarios where perceiving the object’s properties and state is critical for task success. In such cases, tactile feedback becomes essential for manipulation. While the rapid progress of supervised visuomotor policies has benefited greatly from high-quality, reproducible simulation benchmarks in visual imitation, the visuotactile domain still lacks a similarly comprehensive and reliable benchmark for large-scale and rigorous evaluation. To address this, we introduce ManiFeel, a reproducible and scalable simulation benchmark for studying supervised visuotactile manipulation policies across a diverse set of tasks and scenarios. ManiFeel presents a comprehensive benchmark suite spanning a diverse set of manipulation tasks, evaluating various policies, input modalities, and tactile representation methods. Through extensive experiments, our analysis reveals key factors that influence supervised visuotactile policy learning, identifies the types of tasks where tactile sensing is most beneficial, and highlights promising directions for future research in visuotactile policy learning. ManiFeel aims to establish a reproducible benchmark for supervised visuotactile policy learning, supporting progress in visuotactile manipulation and perception. To facilitate future research and ensure reproducibility, we will release our codebase, datasets, training logs, and pre-trained checkpoints. Please visit the project website for more details: <https://zhengtongxu.github.io/manifeel-website/>.

Keywords: Tactile sensing, imitation learning, visuotactile policy learning

1 Introduction

In recent years, supervised policy learning has made significant strides in robot manipulation, where visual input is used to generate actions for long-horizon and complex manipulation tasks [1, 2, 3, 4]. However, such vision-based policies encounter notable limitations in environments where visual cues are absent or severely degraded. For example, in cluttered or confined spaces and under low-light conditions, the visual modality may become unreliable, necessitating alternative sensory inputs to ensure robust task execution. In these scenarios, tactile feedback plays a crucial role, compensating for the limitations of vision by providing contact-based sensory information that can effectively guide manipulation.

Combining visual and tactile modalities has emerged as a promising and intuitive approach for learning robotic manipulation, particularly within supervised policy learning frameworks. Recent studies have shown that integrating high-resolution vision-based tactile sensors, such as Gel-Sight [5], can significantly enhance manipulation performance by providing contact-rich informa-

tion [6, 7, 8, 9, 10]. Various other tactile sensing modalities, such as tactile arrays [11, 12, 13], force-torque sensors [14, 15], tactile 3D point clouds [16], and contact-induced audio signals [17], have also shown strong potential, particularly in tasks requiring fine-grained contact reasoning or operation within unstructured environments.

However, unlike visual imitation learning, which benefits from a wide range of established simulation benchmarks that support large-scale experimentation and statistically meaningful comparisons [18, 19, 20], visuotactile policy learning lacks comparable infrastructure. This gap is largely attributed to the challenges of accurately simulating high-fidelity tactile sensing. The lack of standardized benchmarking tasks and reproducible simulation environments has hindered the systematic development and evaluation of robust visuotactile manipulation policies. Consequently, evaluating the effectiveness of different approaches in a controlled and consistent manner remains a significant challenge. As a result, current research in supervised visuotactile policy learning lacks sufficient comparative analysis [10, 8, 7], limiting our understanding of its core principles and hindering the exploration of promising future directions.

To address these challenges, we introduce ManiFeel, a scalable and reproducible simulation benchmark for supervised visuotactile policy learning. Our contribution can be summarized as follows.

1) **Visuotactile Task Suite:** ManiFeel offers a diverse set of tasks and corresponding human demonstration datasets, including insertion, gear assembly, manipulation inside containers, and tasks performed under dim lighting conditions. These tasks are designed to capture a wide range of contact-rich and perception-challenging scenarios, enabling systematic evaluation of how tactile feedback contributes to multimodal policy learning. ManiFeel provides a comprehensive testbed for studying the strengths and limitations of different sensing modalities and promoting the development of better visuotactile policies.

2) **Modular Policy Architecture Design:** ManiFeel modularizes the visuotactile policy pipeline into three key components: sensing modalities, tactile representations, and policies. This modular design facilitates the integration of diverse policy architectures. By enabling flexible combinations and systematic comparisons across these modules, ManiFeel enables in-depth investigation into which model structures offer greater advantages for visuotactile policy learning.

3) **Empirical Analysis of Visuotactile Policy Learning:** We conduct extensive empirical comparisons on diverse tasks across different policy architectures by systematically varying sensing modalities, tactile representations, and policies. These experiments are conducted in both simulation and real-world settings, allowing us to identify tasks where tactile sensing plays a critical role, uncover effective design choices for visuotactile policy learning, and highlight challenges and promising directions for future research.

4) **Real-world Deployment and Reproduction:** In addition to constructing simulation benchmarks, we also reproduce the results in real-world settings, comparing different policy architectures and sensing modalities. The consistency between real-world and simulation results further validates the high fidelity of our simulated task suite.

To promote future research, we will open-source the ManiFeel codebase, dataset, training logs, and pretrained checkpoints. We expect ManiFeel to support the visuotactile manipulation community in identifying key challenges, benchmarking progress against prior work, and advancing toward robust solutions for a wide range of visuotactile manipulation tasks across diverse scenarios.

2 ManiFeel: Visuotactile Manipulation Learning Benchmark

This section introduces the task suite and modular pipeline design of the ManiFeel benchmark. ManiFeel features a diverse set of manipulation tasks spanning clear-vision conditions to severely degraded or fully occluded visual settings (Section 2.1). The benchmark includes six task categories: tactile sorting in real-world settings, tactile sorting in simulation, tactile exploration and blind insertion in occluded environments, standard insertion tasks, and gear assembly. This results in a total of eight different task setups, including six simulation setups and two real-world setups, as shown in

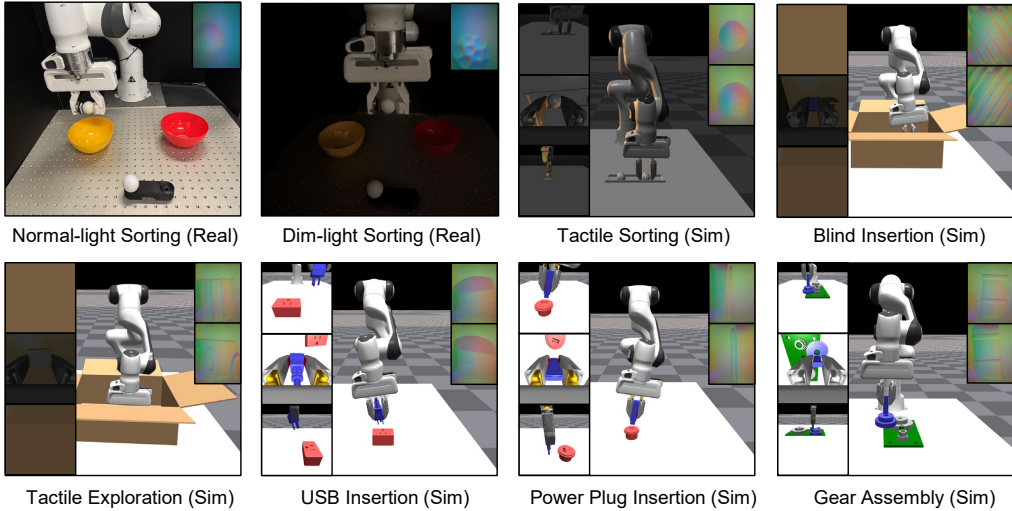


Figure 1: Overview of the manipulation tasks in the ManiFeel benchmark, showing each task’s setup along with the available visual modalities (e.g., wrist camera, agentview camera) and tactile observations (e.g., left and right finger sensors).

Fig. 1. These tasks are designed to vary in their reliance on visual and tactile modalities, providing a comprehensive framework for analyzing policy performance across different sensory challenges. In addition, we describe the modular pipeline design that enables systematic evaluation of different sensing modalities, tactile representations, and policies across the task suite (Section 2.2).

2.1 Task Suite and Dataset

2.1.1 Task and Environment Design

We design a suite of diverse manipulation tasks to systematically evaluate supervised visuotactile policy learning under varying sensory conditions. The tasks are grouped into six categories, reflecting different levels of reliance on visual and tactile modalities (see Fig. 1). In this section, we provide a high-level overview of each task category. Additional details on task configurations and environment setups are provided in the Appendix B.

Tactile Sorting (Real). We introduce a real-world tactile sorting task involving two spherical objects, a table tennis ball and a golf ball, which are visually similar but have distinct surface textures, making them difficult to distinguish using vision alone. The robot must classify each object and move it into its designated bowl. The task is evaluated under two lighting conditions: normal lighting and dim lighting. In this setting, tactile sensing enables robust object classification based on surface texture, highlighting the complementary role of touch when visual information is degraded or ambiguous.

Tactile Sorting (Simulation). The simulated tactile sorting task mirrors the real-world setup in terms of object types and sensory challenges, but differs in its task objective. Instead of sorting balls into bowls, the robot is required to pick up the designated golf ball and lift it to a specified height. The task is performed under dim lighting conditions to emulate reduced visual quality, emphasizing the importance of tactile feedback for reliable object identification when vision alone is insufficient.

Tactile Exploration (Simulation). In this task, the robot must locate, grasp, and lift a cube-shaped battery, which is randomly placed inside a closed container, to a specified height. The external front-facing camera cannot observe the interior, simulating a vision-occluded environment. The

robot relies solely on tactile feedback to explore, localize, and manipulate the object, demonstrating the critical role of touch in environments with severely limited visual information.

Blind Insertion (Simulation). In this task, the robot starts by holding a square peg at an arbitrary orientation and must insert it into a socket located inside a closed container. The external front-facing camera cannot observe the interior, simulating a vision-occluded environment. While the socket pose is fixed, tactile feedback is needed to estimate the in-hand orientation of the peg and to adjust its grasp and alignment for successful insertion under occluded conditions.

Insertion (Simulation). We include insertion tasks that represent fundamental challenges in robotic manipulation, covering standard USB and power plug insertions. The socket location and the in-hand orientation of the objects are randomized at the start of each episode. Successful completion requires leveraging both visual and tactile information to accurately determine the in-hand relative pose and to perform fine adjustments during insertion.

Gear Assembly (Simulation). The gear assembly task simulates an industrial operation where the robot must mount a medium-sized gear onto a central shaft, ensuring correct meshing with side gears. Both the gear base location and in-hand gear orientation are randomized at the start of each episode. The task requires fine spatial alignment, demanding accurate integration of visual and tactile feedback for relative pose estimation and precise adjustment during assembly.

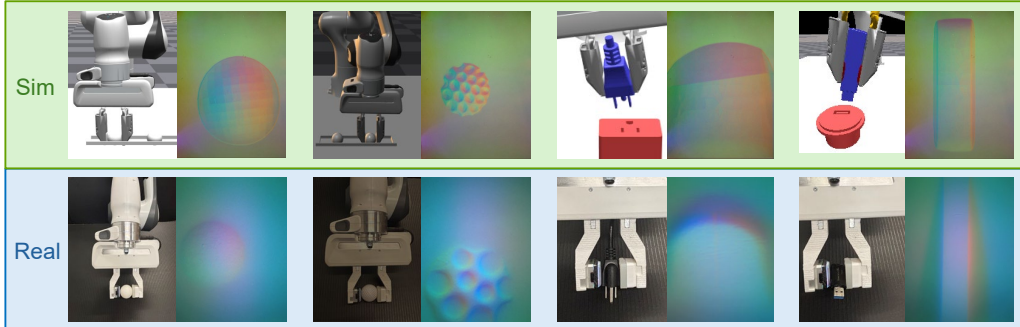


Figure 2: Comparison between tactile images in TacSL simulator [21] and those generated by Gel-Sight Mini. We present examples featuring several objects included in the ManiFeel benchmark.

2.1.2 Observation modalities

ManiFeel is developed on the TacSL simulation platform [21] and supports both vision and tactile observation modalities. For vision, the framework includes multiple camera views and introduces occluded and degraded conditions to emulate realistic manipulation challenges. For tactile sensing, ManiFeel employs a simulated GelSight sensor integrated into a Franka Panda manipulator via TacSL, producing RGB tactile images by measuring surface deformations of a soft elastomer. This setup enables fine-grained perception of object surface geometry during manipulation. Samples of simulated tactile images and their close resemblance to real-world counterparts are shown in Fig. 2, which potentially supports the generalization and applicability of our simulation benchmark to real-world settings. Detailed configurations of camera setups, lighting conditions, and observation modalities for each task are provided in Appendix C.

2.1.3 Teleoperated Demonstration Data Collection

We collect human demonstrations for supervised policy learning using a teleoperation device 3Dconnexion SpaceMouse¹. Tactile feedback plays a critical role during data collection, especially for tasks requiring precise contact understanding or operating under visual occlusion and degraded lighting conditions. In such cases, operators rely heavily on real-time tactile observations displayed on a screen to perceive subtle contact events for effective object grasping, classification, and exploration.

¹<https://3dconnexion.com/us/product/spacemouse-compact/buy/>

We argue that access to tactile information during demonstration is crucial for learning effective visuotactile policies. A summary of the collected demonstration data across all tasks is provided in Appendix C. The collected dataset will be open-sourced to support future research on supervised visuotactile policy learning.

2.2 Modular Pipeline Design

In this section, we present the modular pipeline design that forms the basis of our benchmark. The benchmark is designed to systematically evaluate the performance of visuotactile policies which are composed of different sensing modalities, tactile representations, and policies, across a broad set of tasks. This modular structure enables flexible combinations and fair comparisons, ultimately facilitating a deeper understanding of the design principles behind effective visuotactile policy learning. Moreover, the modularity of our design provides strong flexibility for integrating future advancements, such as new tactile modalities (e.g., force-torque sensing), novel tactile representation learning methods, and emerging policy architectures.

Choice of Modalities. To investigate the contribution of different sensing modalities, we evaluate three configurations: vision-only, tactile-only, and visuotactile. This comparison allows us to isolate the role of each modality and assess how they complement each other in different tasks. By varying the available sensory input, we gain insights into when and how tactile sensing improves policy performance, particularly in contact-rich or visually ambiguous scenarios.

Tactile Representations. We benchmark four types of tactile representations: (1) ResNet18 trained from scratch [1, 22], (2) T3 [10], a pretrained encoder using large-scale tactile datasets, (3) UniT [8], a lightweight representation trained with generalizability, and (4) AnyTouch [23], a generalizable tactile representation learned across diverse sensors and modalities. These comparisons aim to reveal whether pretrained or carefully designed tactile encoders offer meaningful advantages in visuotactile policy learning.

Policies. We compare three types of policies: Diffusion Policy [1], Equivariant Diffusion Policy [24], and Flow Matching [25]. These policies differ in their generative modeling approaches and model architectures. Our goal is to understand how each type of policy performs under different input modalities, and whether certain policies are more compatible with the inclusion of tactile sensing. Specifically, we study how tactile signals influence performance across policy architectures.

3 Experiments

We conduct a comprehensive set of experiments to evaluate the effectiveness of diverse visuotactile policies across diverse manipulation tasks using the ManiFeel simulation benchmark and real-world settings. Our study systematically benchmarks different sensory modalities, tactile representations, and policies under varying task conditions within the supervised policy learning framework. Note that all benchmarking modalities, such as vision, tactile, and visuotactile, also include proprioceptive feedback (i.e., the robot end-effector’s pose). For simulation results, success rates are reported as the primary evaluation metric across all experiments. Specifically, success rates are averaged over the last ten epochs of training, across 50 different environment initializations, and over three seeds. This results in each reported success rate being the average of 1,500 evaluations, providing strong statistical significance. For real-world experiments, we perform 15 consecutive rollouts and record the success rate. The initial environment conditions are varied for each rollout. Through extensive experiments, our analysis reveals key factors that influence supervised visuotactile policy learning, identifies the types of tasks where tactile sensing is most beneficial, and highlights key challenges and promising directions for advancing multimodal robotic manipulation.

3.1 Modality Benchmarking

We evaluate the performance of vision-only policies, tactile-only policies, and visuotactile policies across six manipulation tasks using proposed ManiFeel simulation benchmark. All policies use a ResNet18 tactile encoder trained from scratch, and the policy is based on the Diffusion Policy [1], a

widely adopted and well-established framework for supervised policy learning. In the experimental setup, external occluded camera views are used for the tactile exploration and blind insertion tasks performed inside a closed container. This setting emulates the limited visual information available to humans when operating in similarly vision-occluded environments and highlights the challenges faced by visual perception in such scenarios. Further details regarding training details and observation configurations are provided in Appendices E–F.

Table 1: Success rates (%) averaged over three seeds across different tasks and sensory modalities.

Modality	Tactile Sorting	Tactile Exploration	Blind Insertion	USB Insertion	Power Plug Insertion	Gear Assembly
Vision-only	30.3 ± 3.0	42.9 ± 2.9	29.3 ± 1.8	51.1 ± 1.7	52.3 ± 2.2	43.7 ± 3.6
Tactile-only	39.0 ± 2.8	63.5 ± 2.9	38.7 ± 2.3	2.1 ± 0.8	22.5 ± 1.6	0.6 ± 0.5
Visuotactile	60.8 ± 1.9	55.6 ± 3.5	31.6 ± 1.6	51.4 ± 2.6	55.1 ± 2.8	22.0 ± 2.9

As shown in Table 1, tactile sensing is critical in tasks where visual information is limited or degraded. Specifically, tactile sorting (conducted under dim lighting), tactile exploration, and blind insertion (both performed inside a closed container) show substantial improvements when using tactile-augmented and visuotactile policies compared to the vision-only baseline. For example, in tactile sorting, success rates improve from 30.3% (vision-only) to 39.0% (tactile-only) and further to 60.8% (visuotactile). Similarly, in tactile exploration, performance increases from 42.9% (vision-only) to 63.5% (tactile-only), although visuotactile performance slightly decreases to 55.6%. In blind insertion, tactile-only achieves 38.7% compared to 29.3% with vision-only, while visuotactile reaches 31.6%. These results highlight the importance of tactile feedback in environments where vision becomes unreliable due to poor illumination or occlusion.

For tactile exploration and blind insertion, the tactile-only policy achieves higher success rates than the visuotactile policy. The inclusion of visual input, heavily occluded by the closed container, appears to introduce uninformative signals that degrade policy learning. This observation highlights a key challenge in multimodal learning: the naive integration of noisy or irrelevant modalities can hinder performance, indicating the need for more selective or adaptive sensory fusion strategies.

For gear insertion and assembly tasks, the performance difference between policies with and without tactile input is less pronounced. In USB insertion, success rates are similar between vision-only and visuotactile policies, which are 51.1% and 51.4%, respectively. Power plug insertion exhibits a similar trend, where tactile sensing provides little additional benefit over vision. In the gear assembly task, however, the visuotactile policy performs worse than the vision-only baseline. These results indicate that vision plays a critical role in these tasks, as visual cues such as object pose and geometry are essential for successful manipulation.

For humans, tactile sensing also plays a crucial role in accomplishing insertion and assembly tasks. However, the results show that simply combining tactile and visual inputs within Diffusion Policy does not guarantee improved performance on these tasks. In gear assembly, in particular, the task complexity arising from the need for precise orientation, teeth alignment, and dynamic interaction with rotating side gears creates a highly challenging multimodal observation space. Naively fusing visual and tactile inputs increases the complexity and variability of the policy input, making direct end-to-end learning more challenging and leading to noticeable performance degradation. These results indicate the need for more effective approaches to visuotactile policy learning that can integrate multimodal information more efficiently and enable more robust policies. Our representation benchmarking (Section 3.2, Table 2) supports this view, showing that UniT [8], a carefully designed pretrained tactile representation, improves gear assembly success by over 12 percentage points compared to naive fusion. This suggests that learning structured, generalizable visuotactile representations is a promising direction for advancing multimodal policy learning in complex tasks.

Together, these results demonstrate that while tactile sensing is indispensable in visually challenging conditions, its integration must be carefully managed to maximize its benefits and avoid unintended negative impacts on policy performance. Our ManiFeel benchmark provides a structured

platform for identifying such key challenges and guiding future research on effective visuotactile policy learning. Additional results, including benchmarking with proprioceptive inputs (e.g., robot proprioception) and comparisons across different camera viewpoints for selective tasks, are provided in Appendix F.

3.2 Tactile Representation Benchmarking

We present simulation benchmarking results for visuotactile policies equipped with different tactile representations, as shown in Table 2. In the experimental setup, visual input is incorporated for the tactile sorting and gear assembly tasks, but omitted for tactile exploration, since including uninformative visual signals caused by the occluded view of the closed container, as discussed in Section 3.1, was found to degrade learning performance. The evaluation is conducted across three representative manipulation tasks: tactile sorting, tactile exploration, and gear assembly. ResNet18 encoder is trained from scratch, while UniT [8], T3 [10], and AnyTouch [23] are pre-trained tactile encoders. Further details on the encoder architectures and training details can be found in Appendices D–E.

Table 2: Success rates (%) averaged over three seeds for each task across various tactile-augmented policy structures of different tactile representations. **Bold** indicates best performance.

Task	ResNet18	UniT	T3	AnyTouch
Tactile Sorting	60.8 ± 1.9	50.9 ± 2.9	52.3 ± 2.1	70.4 ± 2.3
Tactile Exploration*	63.5 ± 2.9	59.9 ± 1.8	59.8 ± 2.8	59.8 ± 3.8
Gear Assembly	22.0 ± 2.9	34.5 ± 3.0	25.2 ± 3.0	0.9 ± 0.6

(*) For tactile exploration, the tactile-augmented policy uses only tactile observations without visual input.

AnyTouch achieves the highest success rate on tactile sorting (70.4%) and performs competitively on tactile exploration, demonstrating strong capabilities in tasks that rely on fine contact perception. However, its performance drops considerably on the gear assembly task, suggesting limited generalization to more complex spatial manipulation. In contrast, UniT shows more balanced performance across all tasks, achieving the best result (34.5%) on gear assembly. This highlights the potential of leveraging large-scale pretraining for tactile modalities to enhance supervised visuomotor policy learning. ResNet18, despite being trained from scratch, performs competitively on tactile sorting and tactile exploration tasks, indicating that task-specific training can still be valuable in certain settings. These results suggest that although pre-trained tactile encoders provide strong priors, their effectiveness can vary depending on the specific characteristics of the manipulation task.

Our results further highlight the potential of developing tactile representations that are more specifically tailored to policy learning, aiming for more consistent and superior performance across tasks. Additionally, exploring cross-modal representations that effectively integrate tactile and visual information presents a promising direction for achieving better generalization across diverse domains.

3.3 Policy Benchmarking

In this section, we benchmark three policies: Diffusion Policy (DP) [1], Equivariant Diffusion Policy (EquiDiff) [24], and Flow Matching (FM) [25, 26], across three representative manipulation tasks: tactile sorting, tactile exploration, and gear assembly. Two sensing categories are considered: vision-only policies and tactile-augmented policies where visual input is incorporated for tactile sorting and gear assembly, but not for tactile exploration. For tactile encoder, we use ResNet18 trained from scratch in this experiment. For visual encoder, FM and DP use ResNet18 and EquiDiff uses equivariant ResNet18 [24]. Additional details on the policies and training details can be found in Appendices D–E.

As shown in Table 3, tactile-augmented policies consistently outperform vision-only policies across most tasks. Among all policies, EquiDiff achieves the highest overall performance, particularly excelling in tactile sorting and gear assembly tasks. For instance, in the tactile sorting task, EquiDiff improves from 58.9% (vision-only) to 64.4% when tactile input is incorporated, demon-

Table 3: Success rates (%) averaged over 3 seeds for each task, comparing vision-only policies and tactile-augmented policies where visual input is incorporated for tactile sorting and gear assembly, but not for tactile exploration*. Results are reported across three different policies. Bold indicates best performance.

Task	Vision-only Policy			Tactile-augmented Policy		
	DP	EquiDiff	FM	DP	EquiDiff	FM
Tactile Sorting	30.3 ± 3.0	58.9 ± 3.0	5.2 ± 0.6	60.8 ± 1.9	64.4 ± 3.5	40.9 ± 2.8
Tactile Exploration*	42.9 ± 2.9	43.8 ± 7.8	1.2 ± 1.1	63.5 ± 2.9	47.1 ± 14.5	0.7 ± 0.3
Gear Assembly	43.7 ± 3.6	45.1 ± 3.8	2.5 ± 1.5	22.0 ± 2.9	42.9 ± 4.8	3.3 ± 2.0

(*) For tactile exploration, the tactile-augmented policy uses only tactile observations without visual input.

ing its ability to effectively leverage multimodal sensing. In contrast, FM struggles, especially in vision-only policies, suggesting limitations in handling spatial observability challenges. These results demonstrate the effectiveness of the proposed framework for benchmarking and advancing visuotactile policy learning.

3.4 Real-world Experiment

In this section, we evaluate the tactile sorting task in a real-world setting under two lighting conditions: normal and dim. Experiments are conducted using a Franka Panda manipulator² with a robotic hand integrated with a GelSight Mini³. We benchmark vision-only policies and visuotactile policies with different tactile representations ResNet18 trained from scratch, UniT, and T3. We use Diffusion Policy as the policy. Additional details of the experimental setup can be found in Appendix F.

Table 4: Success rates (%) across 15 trials for the real-world tactile-guided ball sorting task under two lighting scenarios: normal and dim, evaluated across different policy structures. Bold indicates the best performance.

Scenario	Vision	Visuotactile (ResNet18)	Visuotactile (UniT)	Visuotactile (T3)
Normal	33.3	86.7	53.3	80.0
Dim	6.7	33.3	40.0	26.7

Table 4 presents the success rates for the real-world tactile-guided ball sorting task under two lighting conditions. Under normal lighting, the visuotactile policy significantly outperforms the vision-only baseline, achieving 86.7% success compared to 33.3%, highlighting the complementary role of tactile feedback even in visually favorable scenarios. The advantage of tactile sensing becomes more pronounced in dimly lit environments, where the performance of vision-only policy drops sharply to 6.7%. In contrast, policies leveraging the tactile modality maintain consistently better performance, with UniT achieving the highest success rate of 40.0%. These results demonstrate the critical importance of tactile sensing for reliable manipulation in visually degraded environments, and validate the effectiveness of learned tactile encoders in enhancing policy robustness. Notably, the relative performance rankings in the normal lighting condition (ResNet18 > T3 > UniT) are consistent between simulation and real-world experiments, suggesting that our proposed simulation benchmark offers a high-fidelity and reliable environment for studying visuotactile manipulation policy learning.

4 Conclusion

This work presents ManiFeel, a simulation benchmark for advancing supervised visuotactile policy learning. Through extensive experiments across diverse manipulation tasks, we systematically evaluate the effects of sensory modalities, tactile representations, and policy structures on perfor-

²<https://franka.de/products/franka-research-3>

³<https://www.gelsight.com/gelsightmini/>

mance. Results highlight the critical role of tactile sensing in visually degraded environments and the challenges of integrating tactile inputs in vision-dominant tasks. ManiFeel provides a structured platform for benchmarking visuotactile learning and guiding future research toward effective multimodal integration.

5 Limitation

One limitation of our current benchmark is the lack of support for GelSight marker-based tracking as an input modality for learning contact-rich manipulation policies. Although our benchmark covers a range of visuotactile tasks, it does not yet incorporate observations based on marker displacement, which have recently been shown to play a critical role in enabling tactile-reactive and contact-sensitive policies [9]. Existing simulation methods [21, 27] for marker displacement provide a promising starting point for approximating this modality, and future improvements in the fidelity of such simulations may enable more realistic and informative tactile feedback. Building benchmarks that include simulated marker-based signals and systematically evaluating their impact on policy learning could be a promising direction for future work.

References

- [1] C. Chi, S. Feng, Y. Du, Z. Xu, E. Cousineau, B. Burchfiel, and S. Song. Diffusion policy: Visuomotor policy learning via action diffusion. In *Proceedings of Robotics: Science and Systems*, 2023.
- [2] C. Chi, Z. Xu, C. Pan, E. Cousineau, B. Burchfiel, S. Feng, R. Tedrake, and S. Song. Universal manipulation interface: In-the-wild robot teaching without in-the-wild robots. *arXiv preprint arXiv:2402.10329*, 2024.
- [3] T. Z. Zhao, V. Kumar, S. Levine, and C. Finn. Learning fine-grained bimanual manipulation with low-cost hardware. In *Proceedings of Robotics: Science and Systems*, 2023.
- [4] Z. Fu, T. Z. Zhao, and C. Finn. Mobile aloha: Learning bimanual mobile manipulation with low-cost whole-body teleoperation. *arXiv preprint arXiv:2401.02117*, 2024.
- [5] W. Yuan, S. Dong, and E. H. Adelson. GelSight: High-resolution robot tactile sensors for estimating geometry and force. *Sensors*, 2017.
- [6] L. Wang, J. Zhao, Y. Du, E. H. Adelson, and R. Tedrake. Poco: Policy composition from and for heterogeneous robot learning. In *Proceedings of Robotics: Science and Systems*, 2024.
- [7] K. Yu, Y. Han, Q. Wang, V. Saxena, D. Xu, and Y. Zhao. Mimictouch: Leveraging multi-modal human tactile demonstrations for contact-rich manipulation. In *Proceedings of Conference on Robot Learning*, 2024.
- [8] Z. Xu, R. Uppuluri, X. Zhang, C. Fitch, P. G. Crandall, W. Shou, D. Wang, and Y. She. UniT: Data efficient tactile representation with generalization to unseen objects, 2025. URL <https://arxiv.org/abs/2408.06481>.
- [9] H. Xue, J. Ren, W. Chen, G. Zhang, Y. Fang, G. Gu, H. Xu, and C. Lu. Reactive diffusion policy: Slow-fast visual-tactile policy learning for contact-rich manipulation. *arXiv preprint arXiv:2503.02881*, 2025.
- [10] J. Zhao, Y. Ma, L. Wang, and E. H. Adelson. Transferable tactile transformers for representation learning across diverse sensors and tasks. In *Proceedings of Conference on Robot Learning*, 2024.
- [11] I. Guzey, Y. Dai, B. Evans, S. Chintala, and L. Pinto. See to touch: Learning tactile dexterity through visual incentives. In *Proceedings of International Conference on Robotics and Automation*, 2024.
- [12] T. Lin, Y. Zhang, Q. Li, H. Qi, B. Yi, S. Levine, and J. Malik. Learning visuotactile skills with two multifingered hands. In *Proceedings of International Conference on Robotics and Automation*, 2025.

[13] R. Bhirangi, V. Pattabiraman, E. Erciyes, Y. Cao, T. Hellebrekers, and L. Pinto. Anyskin: Plug-and-play skin sensing for robotic touch. *arXiv preprint arXiv:2409.08276*, 2024.

[14] W. Yang, A. Angleraud, R. S. Pieters, J. Pajarinen, and J.-K. Kämäärinen. Seq2seq imitation learning for tactile feedback-based manipulation. In *Proceedings of IEEE International Conference on Robotics and Automation*, pages 5829–5836, 2023.

[15] Y. Hou, Z. Liu, C. Chi, E. Cousineau, N. Kuppuswamy, S. Feng, B. Burchfiel, and S. Song. Adaptive compliance policy: Learning approximate compliance for diffusion guided control. *arXiv preprint arXiv:2410.09309*, 2024.

[16] B. Huang, Y. Wang, X. Yang, Y. Luo, and Y. Li. 3d-vitac: Learning fine-grained manipulation with visuo-tactile sensing. In *Proceedings of Conference on Robot Learning*, 2024. URL <https://openreview.net/forum?id=bk28WlkqZn>.

[17] Z. Liu, C. Chi, E. Cousineau, N. Kuppuswamy, B. Burchfiel, and S. Song. Maniaw: Learning robot manipulation from in-the-wild audio-visual data. *arXiv preprint arXiv:2406.19464*, 2024.

[18] A. Mandlekar, D. Xu, J. Wong, S. Nasiriany, C. Wang, R. Kulkarni, L. Fei-Fei, S. Savarese, Y. Zhu, and R. Martín-Martín. What matters in learning from offline human demonstrations for robot manipulation. In *Proc. Conf. Robot Learn.*, pages 1678–1690, 2022.

[19] A. Mandlekar, S. Nasiriany, B. Wen, I. Akinola, Y. Narang, L. Fan, Y. Zhu, and D. Fox. Mimicgen: A data generation system for scalable robot learning using human demonstrations. *arXiv preprint arXiv:2310.17596*, 2023.

[20] S. Tao, F. Xiang, A. Shukla, Y. Qin, X. Hinrichsen, X. Yuan, C. Bao, X. Lin, Y. Liu, T.-k. Chan, et al. Maniskill3: Gpu parallelized robotics simulation and rendering for generalizable embodied ai. *arXiv preprint arXiv:2410.00425*, 2024.

[21] I. Akinola, J. Xu, J. Carius, D. Fox, and Y. Narang. Tacsl: A library for visuotactile sensor simulation and learning. *IEEE Transactions on Robotics*, 41:2645–2661, 2025. doi:10.1109/TRO.2025.3547267.

[22] K. He, X. Zhang, S. Ren, and J. Sun. Deep residual learning for image recognition. In *Proc. IEEE Conf. Comput. Vis. Pattern Recognit.*, 2016.

[23] R. Feng, J. Hu, W. Xia, T. Gao, A. Shen, Y. Sun, B. Fang, and D. Hu. Anytouch: Learning unified static-dynamic representation across multiple visuo-tactile sensors. *arXiv preprint arXiv:2502.12191*, 2025.

[24] D. Wang, S. Hart, D. Surovik, T. Kelestemur, H. Huang, H. Zhao, M. Yeatman, J. Wang, R. Walters, and R. Platt. Equivariant diffusion policy. *arXiv preprint arXiv:2407.01812*, 2024.

[25] F. Zhang and M. Gienger. Affordance-based robot manipulation with flow matching. *arXiv preprint arXiv:2409.01083*, 2024.

[26] K. Black, N. Brown, D. Driess, A. Esmail, M. Equi, C. Finn, N. Fusai, L. Groom, K. Hausman, B. Ichter, et al. π 0: A vision-language-action flow model for general robot control, 2024. URL <https://arxiv.org/abs/2410.24164>, 2024.

[27] J. Xu, S. Kim, T. Chen, A. R. Garcia, P. Agrawal, W. Matusik, and S. Sueda. Efficient tactile simulation with differentiability for robotic manipulation. In *Proceedings of Conference on Robot Learning*, 2022. URL <https://openreview.net/forum?id=6BIffC16gsM>.

[28] C. Wang, H. Shi, W. Wang, R. Zhang, L. Fei-Fei, and C. K. Liu. Dexcap: Scalable and portable mocap data collection system for dexterous manipulation. *arXiv preprint arXiv:2403.07788*, 2024.

[29] S. Lee, Y. Wang, H. Etukuru, H. J. Kim, N. M. M. Shafiullah, and L. Pinto. Behavior generation with latent actions. *arXiv preprint arXiv:2403.03181*, 2024.

[30] O. M. Team, D. Ghosh, H. Walke, K. Pertsch, K. Black, O. Mees, S. Dasari, J. Hejna, C. Xu, J. Luo, et al. Octo: An open-source generalist robot policy, 2023.

[31] T. Z. Zhao, J. Tompson, D. Driess, P. Florence, K. Ghasemipour, C. Finn, and A. Wahid. Aloha unleashed: A simple recipe for robot dexterity. *arXiv preprint arXiv:2410.13126*, 2024.

[32] Y. Ze, G. Zhang, K. Zhang, C. Hu, M. Wang, and H. Xu. 3D diffusion policy. In *Proceedings of Robotics: Science and Systems*, 2024.

[33] Z. Xue, S. Deng, Z. Chen, Y. Wang, Z. Yuan, and H. Xu. Demogen: Synthetic demonstration generation for data-efficient visuomotor policy learning. *arXiv preprint arXiv:2502.16932*, 2025.

[34] F. R. Hogan, J. Ballester, S. Dong, and A. Rodriguez. Tactile Dexterity: Manipulation primitives with tactile feedback. In *Proc. IEEE Int. Conf. Robot. Autom.*, pages 8863–8869, 2020.

[35] S. Kim and A. Rodriguez. Active extrinsic contact sensing: Application to general peg-in-hole insertion. In *Proc. IEEE Int. Conf. Robot. Autom.*, pages 10241–10247, 2022.

[36] Y. Shirai, D. K. Jha, A. U. Raghunathan, and D. Hong. Tactile tool manipulation. *arXiv preprint arXiv:2301.06698*, 2023.

[37] Y. Du, P. Zhou, M. Y. Wang, W. Lian, and Y. She. Stick roller: A case study on efficiently learning precise tactile dynamics for in-hand manipulation. In *Proceedings of IEEE/RSJ International Conference on Intelligent Robots and Systems*, pages 2312–2318, 2024.

[38] Y. She, S. Wang, S. Dong, N. Sunil, A. Rodriguez, and E. Adelson. Cable manipulation with a tactile-reactive gripper. *Int. J. Robot. Res.*, 40(12-14):1385–1401, 2021.

[39] N. Sunil, S. Wang, Y. She, E. Adelson, and A. R. Garcia. Visuotactile affordances for cloth manipulation with local control. In *Proc. Conf. Robot Learn.*, 2022.

[40] S. Aslam, K. Kumar, P. Zhou, H. Yu, M. Yu Wang, and Y. She. Dartbot: Overhand throwing of deformable objects with tactile sensing and reinforcement learning. *IEEE Transactions on Automation Science and Engineering*, 22:13644–13661, 2025. [doi:10.1109/TASE.2025.3556875](https://doi.org/10.1109/TASE.2025.3556875).

[41] Z. Zhao, Y. Li, W. Li, Z. Qi, L. Ruan, Y. Zhu, and K. Althoefer. Tac-man: Tactile-informed prior-free manipulation of articulated objects. *IEEE Transactions on Robotics*, 2024.

[42] S. Tian, F. Ebert, D. Jayaraman, M. Mudigonda, C. Finn, R. Calandra, and S. Levine. Manipulation by Feel: Touch-based control with deep predictive models. In *Proc. IEEE Int. Conf. Robot. Autom.*, pages 818–824, 2019.

[43] Y. Zheng, F. F. Veiga, J. Peters, and V. J. Santos. Autonomous learning of page flipping movements via tactile feedback. *IEEE Transactions on Robotics*, 38(5):2734–2749, 2022.

[44] Z. Xu and Y. She. LeTac-MPC: Learning model predictive control for tactile-reactive grasping. *IEEE Transactions on Robotics*, 2024. [doi:10.1109/TRO.2024.3463470](https://doi.org/10.1109/TRO.2024.3463470).

[45] J. Lloyd and N. F. Lepora. Goal-driven robotic pushing using tactile and proprioceptive feedback. *IEEE Transactions on Robotics*, 38(2):1201–1212, 2021.

[46] R. Calandra, A. Owens, M. Upadhyaya, W. Yuan, J. Lin, E. H. Adelson, and S. Levine. The Feeling of Success: Does touch sensing help predict grasp outcomes? In *Proc. Conf. Robot Learn.*, pages 314–323, 2017.

[47] Z. Si, Z. Zhu, A. Agarwal, S. Anderson, and W. Yuan. Grasp stability prediction with sim-to-real transfer from tactile sensing. In *Proc. IEEE/RSJ Int. Conf. Intell. Robots Syst.*, pages 7809–7816, 2022.

[48] S. Kanitkar, H. Jiang, and W. Yuan. PoseIt: A visual-tactile dataset of holding poses for grasp stability analysis. In *Proc. IEEE/RSJ Int. Conf. Intell. Robots Syst.*, pages 71–78, 2022.

[49] R. Calandra, A. Owens, D. Jayaraman, J. Lin, W. Yuan, J. Malik, E. H. Adelson, and S. Levine. More Than a Feeling: Learning to grasp and regrasp using vision and touch. *IEEE Robotics and Automation Letters*, 3(4):3300–3307, 2018.

[50] F. R. Hogan, M. Bauza, O. Canal, E. Donlon, and A. Rodriguez. Tactile Regrasp: Grasp adjustments via simulated tactile transformations. In *Proc. IEEE/RSJ Int. Conf. Intell. Robots Syst.*, pages 2963–2970, 2018.

[51] Q. Feng, Z. Chen, J. Deng, C. Gao, J. Zhang, and A. Knoll. Center-of-mass-based robust grasp planning for unknown objects using tactile-visual sensors. In *Proc. IEEE Int. Conf. Robot. Autom.*, pages 610–617, 2020.

[52] Y. Han, R. Batra, N. Boyd, T. Zhao, Y. She, S. Hutchinson, and Y. Zhao. Learning generalizable vision-tactile robotic grasping strategy for deformable objects via transformer. *arXiv preprint arXiv:2112.06374*, 2021.

[53] M. Polic, I. Krajacic, N. Lepora, and M. Orsag. Convolutional autoencoder for feature extraction in tactile sensing. *IEEE Robotics and Automation Letters*, 4(4):3671–3678, 2019.

[54] C. Sferrazza, Y. Seo, H. Liu, Y. Lee, and P. Abbeel. The power of the senses: Generalizable manipulation from vision and touch through masked multimodal learning. In *Proceedings of IEEE/RSJ International Conference on Intelligent Robots and Systems*, 2024.

[55] G. Cao, J. Jiang, D. Bollegala, and S. Luo. Learn from incomplete tactile data: Tactile representation learning with masked autoencoders. In *Proceedings of IEEE/RSJ International Conference on Intelligent Robots and Systems*, pages 10800–10805, 2023.

[56] C. Higuera, A. Sharma, et al. Sparsh: Self-supervised touch representations for vision-based tactile sensing. In *Proceedings of Conference on Robot Learning*, 2024.

[57] H. Gupta, Y. Mo, S. Jin, and W. Yuan. Sensor-invariant tactile representation. *arXiv preprint arXiv:2502.19638*, 2025.

[58] F. Yang et al. Binding touch to everything: Learning unified multimodal tactile representations. In *Proceedings of the IEEE/CVF Conference on Computer Vision and Pattern Recognition*, pages 26340–26353, 2024.

Appendix

A Related Work

A.1 Imitation Learning

In recent years, imitation learning has progressed rapidly, enabling robots to perform complex, dexterous, and long-horizon manipulation within supervised learning paradigm [1, 2, 3, 4]. Different lines of work have focused on various aspects of imitation learning, such as novel data collection pipelines [3, 4, 28], the design of diverse policy heads such as diffusion [1], flow matching [25], and VQVAE [29], and the development of large-scale policies by integrating vision-language models [26] or scaling up both dataset and model capacity [30, 31].

Traditional imitation learning has predominantly relied on visual modalities, such as images [1, 2, 3] or 3D point clouds [32, 33]. Moreover, visuotactile imitation learning has attracted growing attention. Since manipulation inherently involves interactions with the environment, tactile sensing provides complementary information that is crucial for capturing these interactions. As such, combining visual and tactile modalities to learn manipulation policies via imitation learning has become a natural and promising direction. For instance, several works have leveraged high-resolution vision-based tactile sensors such as GelSight [5], which provide rich contact information and have led to notable improvements in policy learning [6, 7, 8, 9]. In parallel, other tactile modalities, including tactile arrays [11, 12, 13], force-torque sensors [14, 15], tactile 3D point cloud [16], and audio sensors [17], have also demonstrated strong performance, particularly in tasks involving fine-grained manipulation and complex environment interactions.

However, unlike visual imitation learning, which benefits from a wide range of established policy learning benchmarks, tactile sensing remains difficult to simulate accurately in existing robotic simulators. As a result, most prior works report results directly in real-world environments, without simulation-based benchmarks. Yet, simulation benchmarks offer significant advantages: they allow for extensive rollouts across diverse environments and enable consistent evaluation throughout training, leading to more statistically meaningful comparisons and insights into learning trends. This is particularly valuable for understanding the role of tactile feedback in imitation learning.

Despite this potential, there is currently a lack of simulation benchmarks tailored to visuotactile policy learning. To address this gap, we introduce a new benchmark specifically designed for evaluating supervised visuotactile policy learning in simulated settings.

A.2 Visuotactile Manipulation

Tactile feedback has been widely explored for manipulation tasks involving rigid [34, 35, 36, 37], deformable [38, 39, 40], and articulated objects [41]. A common strategy is to extract low-level state estimations, such as contact areas or object pose, from tactile signals to guide model-based controllers. Moreover, some approaches integrate tactile signals into model predictive control frameworks [42], or into task-specific solutions like page flipping [43], grasping [44], robotic pushing [45]. Finally, learning-based tactile control frameworks have emerged to improve adaptability. For instance, neural networks have been used to predict grasp stability or success [46, 47, 48], and to evaluate candidate actions by sampling-based method [49, 50, 51, 52].

The aforementioned works focus on modeling specific tasks or object categories by incorporating visuotactile information, and subsequently designing manipulation policies. However, the resulting policies or controllers are typically task-specific, and their pipelines often struggle to generalize to other tasks or object types. In contrast, imitation learning offers a more general and flexible approach by learning manipulation policies directly from demonstration data, making it more adaptable to a broader range of tasks and objects.

A.3 Tactile Representation Learning

Recent advances in tactile representation learning span a wide range of approaches. Some studies leverage convolutional neural networks to extract features directly from tactile signals [53], while others use masked autoencoding methods for more structured representation learning [54, 55]. The work in [8] employs VQGAN to learn a generalizable efficient tactile representation using very simple object dataset. In parallel, growing efforts have focused on developing transferable representations across diverse tactile sensors and perception tasks [56, 10]. The study in [57] introduces a sensor-invariant tactile representation by incorporating a normal map reconstruction loss. Notably, [58, 23] propose multimodal representations by grounding tactile signals in pretrained foundation models, enabling improved generalization across modalities.

Most of the existing tactile representation learning works evaluate their methods on downstream perception tasks such as classification and pose estimation, as these benchmarks are relatively easy to set up and require low data collection costs. In contrast, a fair and comprehensive comparison of different tactile representations in the context of policy learning is equally important but less explored. Our benchmark enables such evaluation by providing a standardized and scalable framework for policy learning with tactile representations.

B Additional Details on Task Environments

This section provides additional environment configuration details for each task used in our real-world and simulation experiments. All task setups are built upon the IsaacGym simulation⁴. The code and configuration files for all simulation task setups will be open-sourced to facilitate reproducibility.

Tactile Sorting (Real). The robot must classify and sort two visually similar spherical objects, a golf ball and a table tennis ball, into red and yellow bowls, respectively. The task is conducted under either normal or dim lighting conditions. Visual observations are captured using a front-facing Intel RealSense camera⁵, while tactile feedback is provided by a GelSight Mini sensor mounted on the robot’s gripper. The two balls are placed on a ball stand. At the start of every new demonstration or evaluation rollout, the positions of the two balls are swapped to introduce the variation. OSC-yaw controller is used to control end-effector position and yaw rotation, while roll and pitch are kept fixed throughout the execution.

Tactile Sorting (Simulation). This task is conducted under dim lighting conditions to simulate degraded visual perception. A golf ball and a table tennis ball are placed on a ball stand whose position is randomly initialized within a range of $(-5 \text{ cm}, +5 \text{ cm})$ along both x and y axes from its nominal position at the start of each demonstration or evaluation rollout. To increase task diversity, the positions of the balls (i.e., golf vs. table tennis) are also swapped between different episodes.

Tactile Exploration (Simulation). This task is performed in a vision-occluded environment, with the object (a cube-shaped battery) placed inside a closed container. At the beginning of each demonstration or evaluation, the object’s position is randomly placed at two predefined locations along the x -axis. Due to the limited and occluded visual input, the robot must rely solely on tactile feedback for object exploration, localization, and grasping.

Blind Insertion (Simulation). In this vision-occluded task, the socket’s position remains fixed throughout all rollouts, while the peg’s initial in-hand orientation is randomized up to 45° . This variation necessitates that the policy infer and adjust the in-hand pose through tactile sensing to ensure successful insertion. In this task, the gripper remains closed to ensure a stable hold on the peg during insertion.

Insertion Tasks (Simulation). For USB and power plug insertion tasks, both the socket location and the in-hand orientation of the object (USB or plug) are randomized at the start of each rollout.

⁴<https://github.com/isaac-sim/IsaacGymEnvs.git>

⁵<https://www.intelrealsense.com/depth-camera-d435/>

The socket position is sampled within a $(-5 \text{ cm}, +5 \text{ cm})$ range along the x and y axes, and the object’s orientation is randomized within 45° of its nominal pose. In this task, the gripper remains closed to ensure a stable hold on the peg during insertion.

Gear Assembly (Simulation). In this industrial-style assembly task, the gear base location on the table and the in-hand orientation of the gear are both randomized at the start of each rollout. The gear base is perturbed within a $(-5 \text{ cm}, +5 \text{ cm})$ range in the $x-y$ plane, and the gear’s initial orientation is randomized within 45° of its nominal pose. In this task, the gripper remains closed to maintain a stable grasp on the gear during precise alignment and placement.

C Dataset Details

We collect expert demonstrations using a 3Dconnexion SpaceMouse for all tasks in the ManiFeel benchmark, including six simulated tasks and one real-world task under two lighting conditions. Table 5 summarizes the amount of demonstrations, camera views, tactile sensors, and action dimensions (ActD) recorded per task. Tasks with an action dimension (ActD) of 7 include gripper open/close actions, while those with an ActD of 6 use a fixed gripper state, which is excluded from the action space.

Each simulation task is recorded with three RGB camera views (front, side, wrist) and two tactile sensors (left and right fingers), whereas the real-world setup includes a front-facing Intel RealSense camera and a single GelSight tactile sensor on the left finger. While not all camera views and tactile sensors are required as inputs during policy training, our dataset captures diverse sensor observations to support flexible usage in future research. The specific observation setup used for ManiFeel policy training is described in Appendix F.

The demonstrations are recorded at 10 Hz and include synchronized visual, tactile, and proprioceptive observations. The proprioceptive feedback includes the end-effector’s position and orientation, resulting in a 7-dimensional state vector, where orientation is represented using a quaternion.

Table 5: **Dataset Summary.** Cam: number of camera viewpoints recorded in the dataset; Tac: number of tactile sensors recorded; PropD: proprioceptive feedback dimension; ActD: action dimension; Demo: number of human demonstrations collected.

Task	Cam	Tac	PropD	ActD	Demo
Simulation Dataset					
Tactile Sorting	3	2	7	7	51
Tactile Exploration	3	2	7	7	41
Blind Insertion	3	2	7	6	51
USB Insertion	3	2	7	6	61
Power Plug Insertion	3	2	7	6	101
Gear Assembly	3	2	7	6	21
Real-world Dataset					
Tactile Sorting (Normal)	1	1	7	5	103
Tactile Sorting (Dim)	1	1	7	5	80

Representative examples of the demonstration trajectories are visualized in Fig. 3. In these scenarios, where visual input alone is often insufficient due to occlusions or degraded lighting, operators rely on real-time tactile images displayed on a monitor to guide precise behaviors, such as identifying surface properties for object classification or estimating in-hand pose for alignment. For instance, in the tactile sorting task under dim lighting, human operators struggle to distinguish between visually similar objects like a table tennis ball and a golf ball. Tactile feedback enables operators to detect surface texture differences and correct initial grasping errors. These observations highlight the importance of tactile input not only for effective teleoperation but also for collecting high-quality data

to support supervised visuotactile policy learning. All of the collected datasets will be open-sourced to support future research in supervised visuotactile policy learning.

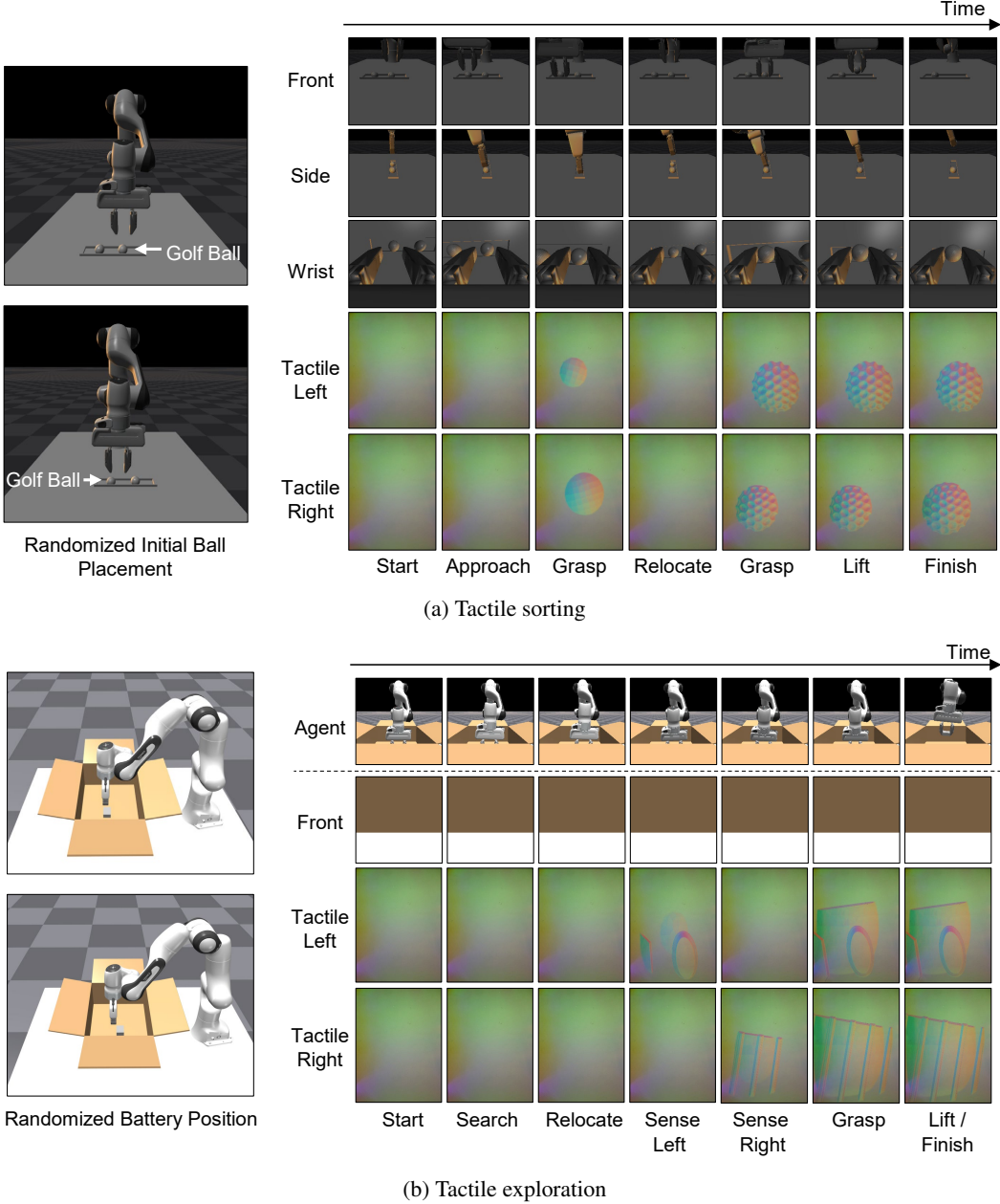


Figure 3: Samples of teleoperated demonstration data in simulation for two representative tasks: (a) tactile sorting and (b) tactile exploration, highlighting scenarios with severely degraded or occluded visual input.

D Pipeline Details

D.1 Visual Encoder

We adopt a ResNet18 CNN encoder (without pretraining) with two key modifications as described in [1]: (1) the global average pooling layer is replaced with a spatial softmax pooling layer to retain spatial information; and (2) Batch Normalization is replaced with Group Normalization to ensure

stable training. Each camera view is processed using a separate encoder. For visuotactile policies that do not rely on pretrained tactile representations, the same ResNet18 encoder is also used to extract features from tactile images.

D.2 Tactile Representations

UniT [8] is a tactile representation model that can be trained on a small set of simple objects while generalizing to unseen objects. It adopts the training paradigm of VQGAN. During inference, the quantization layer is removed from the encoding process, and only the CNN-based downsampling is used for feature extraction. The resulting UniT representation exhibits a well-structured latent space that emphasizes informative tactile features.

UniT is not a representation pretrained on broad datasets, but rather a method designed for domain generalization using only a small amount of task-specific data. The checkpoint released by UniT [8] was trained on GelSight images with markers, which differ from the tactile observations used in ManiFeel. Therefore, we trained customized UniT representations using data of our domain. For the simulation benchmark, we trained UniT using a set of images of nut and bolt collected through TacSL [21], and used the same representation across all simulation experiments. For real-world experiments, we trained UniT with a set of table tennis ball and golf ball images. The UniT encoder contains 75 M parameters.

T3 [10] is built upon vision transformer backbone and is pre-trained on a large-scale dataset collected from multiple tactile sensors. The pretraining includes both masked autoencoding for reconstruction and supervision on perception-related downstream tasks. The resulting representation demonstrates strong generalization and broad applicability across diverse tasks and sensors. We use the T3-medium encoder released by T3 [3] for both simulation and real-world experiments. The model contains 86 M parameters.

AnyTouch [23] is also a tactile representation built upon vision transformer backbone. It is pre-trained on dataset that includes aligned tactile images and videos collected from four different visuotactile sensors. AnyTouch jointly leverages pixel-level reconstruction and multi-sensor alignment objectives to learn semantic features. It enables robust perception and effective cross-sensor transfer, demonstrating strong generalization across both static and dynamic tasks. We use the checkpoint released by AnyTouch [23] for both simulation and real-world experiments. The model’s encoder is based on a ViT-Large backbone, with a total of 305 M parameters. As shown in Table 8, the large size of AnyTouch significantly slows down training for policies, reducing its flexibility.

D.3 Policies

Diffusion Policy [1] formulates action generation as a conditional denoising diffusion process. During training, Gaussian noise is progressively added to ground-truth action sequences to construct a forward diffusion process. A denoising model is then trained to reverse this process by predicting noises, conditioned on visual observations. At inference time, the model performs iterative denoising to sample action sequences, enabling robust and multimodal policy learning from demonstration data. We use CNN-based Diffusion Policy, where the denoising model is a 1D UNet [1].

Equivariant Diffusion Policy [24] extends the diffusion framework by incorporating $SO(2)$ equivariance into both the observation and action representations. This equivariant design enhances generalization and data efficiency, particularly in 6-DoF manipulation tasks exhibiting rotational symmetries. We adopt the image-based Equivariant Diffusion Policy, as all policies operate on RGB visual observations. Additionally, we use the relative control mode of EquiDiff, since both the simulation and real-world environments use a relative action space.

Flow Matching [25] reformulates trajectory generation as learning a continuous flow field that maps random waypoints to actions in a single step. Unlike diffusion models, it avoids iterative denoising by solving an optimal transport-inspired regression problem. This one-shot inference process enables faster policy execution while maintaining comparable performance to diffusion-based methods in many robotic manipulation benchmarks.

E Training Details

Table 6: **Hyperparameters for training and inference.** To: observation horizon; Ta: action horizon; Tp: action prediction horizon; ImgRes: environment RGB image resolution; TacImgRes: tactile image resolution; Lr: learning rate; DiffT.: number of training diffusion iterations; DiffE.: number of inference diffusion iterations.

H-Param	To	Ta	Tp	ImgRes	TacImgRes	Lr	DiffT	DiffE
Tactile Sorting	2	8	16	256x256	256x256	1e-4	100	100
Tactile Exploration	2	8	16	256x256	256x256	1e-4	100	100
Blind Insertion	2	8	16	256x256	256x256	1e-4	100	100
USB Insertion	2	8	16	256x256	256x256	1e-4	100	100
Power Plug Insertion	2	8	16	256x256	256x256	1e-4	100	100
Gear Assembly	2	8	16	256x256	256x256	1e-4	100	100
Real Sorting (Normal)	2	6	16	320x240	320x240	1e-4	75	16
Real Sorting (Dim)	2	8	16	320x240	320x240	1e-4	75	16

We summarize the training and inference hyperparameters in Table 6, which are consistent across all policies. The original visual image resolution is 256×256 , while the tactile images are captured at 240×320 . For training, we consistently resize tactile images to 256×256 when using the ResNet18 tactile encoder and UniT tactile representation, while visual inputs are maintained at 256×256 for the visual encoder. For T3 and AnyTouch, we use 224×224 tactile image inputs to match the ViT backbone architecture. For Diffusion Policy, we adopt DDPM for simulation experiments and switch to DDIM during real-world experiments to enable faster inference. For Equivariant Diffusion Policy, we use DDIM.

F Additional Details on Experiments

F.1 Task Setup

Table 7 summarizes the task configurations used for policy training and evaluation in both simulation and real-world experiments, including the number of cameras, tactile sensors, and training datasets per task. In all experiments, only tactile images from the left finger sensor are used. Tasks with an action dimension (ActD) of 7 include gripper open/close actions, while those with an ActD of 6 use a fixed gripper state, which is excluded from the action space. For real-world experiments, we use an OSC-yaw controller that controls end-effector position and yaw rotation, while roll and pitch are kept fixed throughout the execution. All code and configuration files for training and rollout will be open-sourced to facilitate reproducibility of the results.

Table 7: **Tasks Setup in the Experiments.** Ctrl: control type; Cam: number of cameras; Tac: number of tactile sensors; ActD: action dimension; Demo: number of demonstrations used for training; Lighting: lighting condition; Occlusion: whether the camera view is occluded.

Task	Ctrl	Cam	Tac	ActD	Demo	Lighting	Occlusion
Simulation experiment							
Tactile Sorting	Relative Pose	1 (Front)	1	7	50	Dim	No
Tactile Exploration	Relative Pose	1 (Front)	1	7	40	Normal	Yes
Blind Insertion	Relative Pose	1 (Front)	1	6	30	Normal	Yes
USB Insertion	Relative Pose	1 (Wrist)	1	6	60	Normal	No
Power Plug Insertion	Relative Pose	1 (Wrist)	1	6	90	Normal	No
Gear Assembly	Relative Pose	1 (Wrist)	1	6	20	Normal	No
Real-world experiment							
Tactile Sorting (normal)	Relative Pose	1	1	5	103	Normal	No
Tactile Sorting (dim)	Relative Pose	1	1	5	80	Dim	No

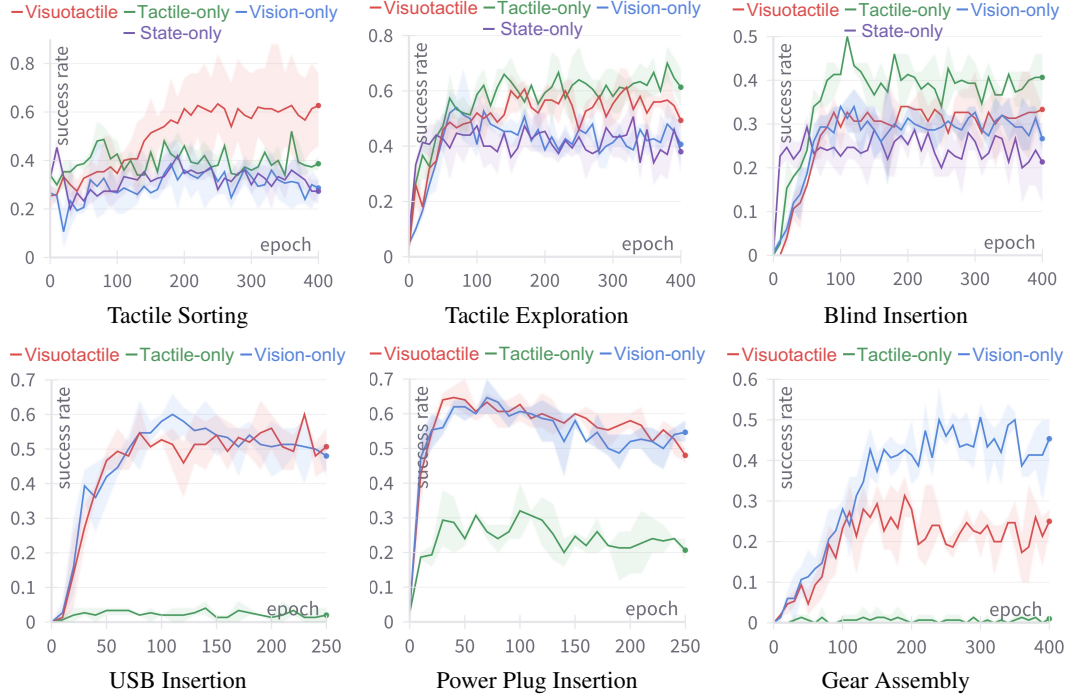


Figure 4: Learning curves comparing sensing modalities across six manipulation tasks. Each plot shows success rates over training epochs. The first row includes tactile sorting, tactile exploration, and blind insertion, where all four sensory configurations are evaluated: visuotactile, tactile-only, vision-only, and state-only. The second row includes USB insertion, power plug insertion, and gear assembly, where only visuotactile, tactile-only, and vision-only configurations are evaluated. Note that all visuotactile, tactile-only, and vision-only policies also include proprioceptive state inputs.

F.2 Learning Curves

In this section, we present learning curves that show success rates over training epochs for all experiments reported in Section 3. Each curve represents the mean success rate across three random seeds (solid line), and the shaded region denotes the range between the maximum and minimum values at each epoch. Policies are evaluated every 10 epochs using 50 different environment initializations to ensure statistical robustness. Figure 4 presents the learning curves from the modality benchmarking experiment (Section 3.1), comparing vision-only, tactile-only, and visuotactile inputs across all six ManiFeel tasks. For tactile sorting, tactile exploration, and blind insertion, we additionally evaluate a state-only policy to analyze the contribution of proprioceptive feedback. The state-only input refers to the 7-dimensional proprioceptive feedback of the end-effector pose (position and orientation), which is also included in all other sensing modality configurations. Notably, for tactile exploration and blind insertion, where visual input is severely occluded, the vision-only and state-only policies perform similarly, suggesting that the performance in vision-only settings is largely driven by proprioceptive input rather than visual cues. Figs. 5 and 6 present learning curves for the tactile representation (Section 3.2) and policy benchmarking (Section 3.3) experiments, respectively, across three representative tasks: tactile sorting, tactile exploration, and gear assembly.

F.3 Runtime Analysis of Tactile Representations

In this section, we evaluate the training time required for different tactile encoders and representations, including ResNet18, UniT, T3, and AnyTouch. Table 8 summarizes the training time per epoch and total training time (over 20 epochs) for visuotactile policies in the real-world sorting task under normal lighting. All experiments are conducted using an NVIDIA A30 GPU with a batch size of 8. AnyTouch incurs substantially higher computational cost, with each training epoch taking

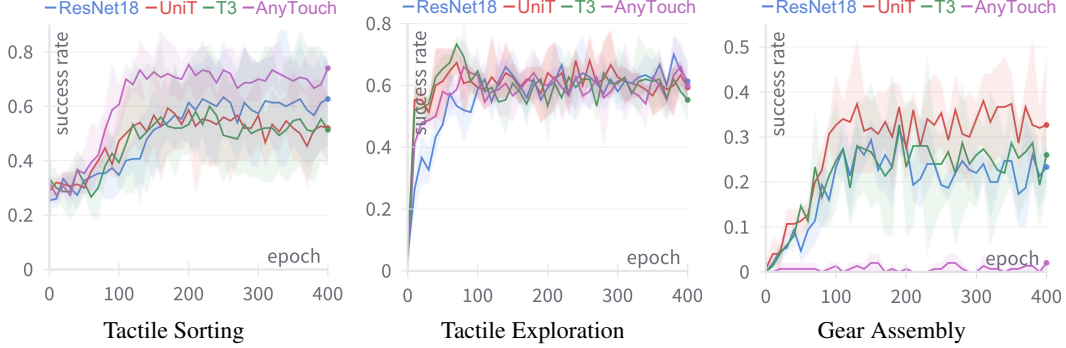


Figure 5: Learning curves across tactile-augmented policies using different tactile representations, for three representative tasks, including tactile sorting, tactile exploration, and gear assembly. For the tactile exploration task, the policy uses only tactile observations without visual input.

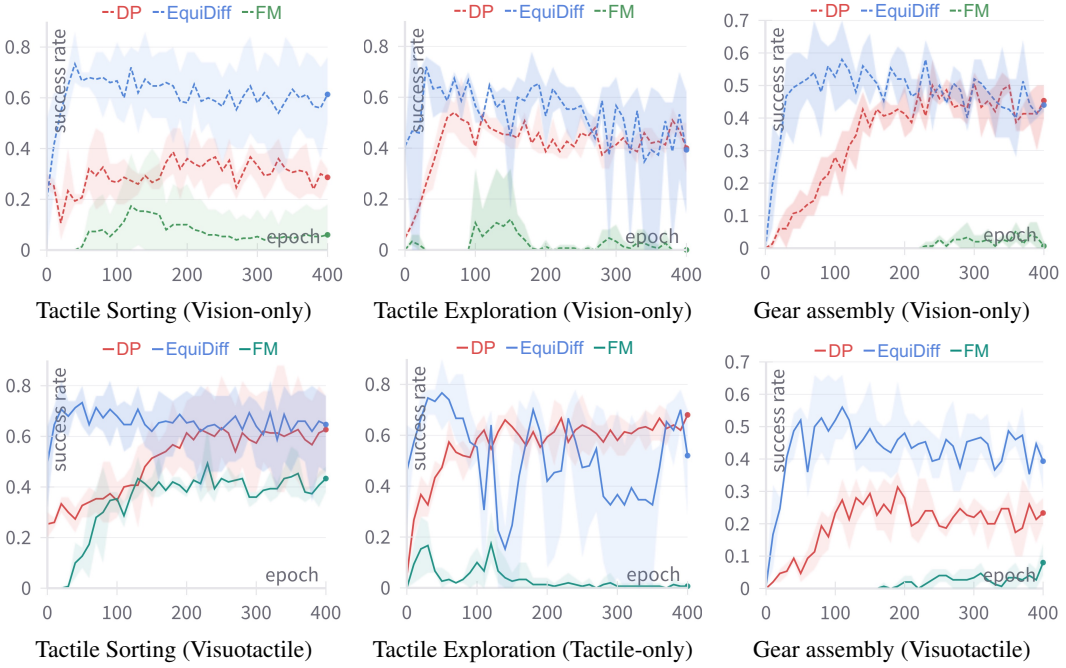


Figure 6: Learning curves for three representative tasks, including tactile sorting, tactile exploration, and gear assembly, evaluated across different policy architectures. Top: vision-only policy. Bottom: tactile-augmented policy, where visual input is included for tactile sorting and gear assembly, but excluded for tactile exploration.

over 67 minutes. In contrast, UniT and T3 are more efficient, with training times of approximately 26 and 18 minutes per epoch, respectively, making them better suited for faster policy iteration and development.

E.4 Experiment on Different Camera Viewpoints

Fig. 7 illustrates the performance of policies in the tactile exploration task when using visual observations from different camera viewpoints, specifically wrist-mounted and front-facing perspectives. Fig. 7a illustrate tactile inputs and visual images from occluded front views and dim wrist views. The results (Figs. 7b–7c) show that both vision-only and visuotactile policies achieve higher success rates when trained with wrist-mounted inputs. Moreover, the visuotactile policy consistently outperforms its vision-only counterpart under both viewpoints, demonstrating that incorporating tactile sensing enhances performance under visually limited conditions.

Table 8: Average training time per epoch and total training time (over 20 epochs) for visuotactile policies with different tactile representations in the real-world sorting task under normal lighting conditions. The dataset includes 103 human demonstrations. Time per epoch is reported in minutes and total time in hours.

Metric	ResNet18	UniT	T3	AnyTouch
Time per Epoch (min)	8.1	25.8	17.7	66.3
Total Time (hr)	2.7	8.6	5.9	22.1

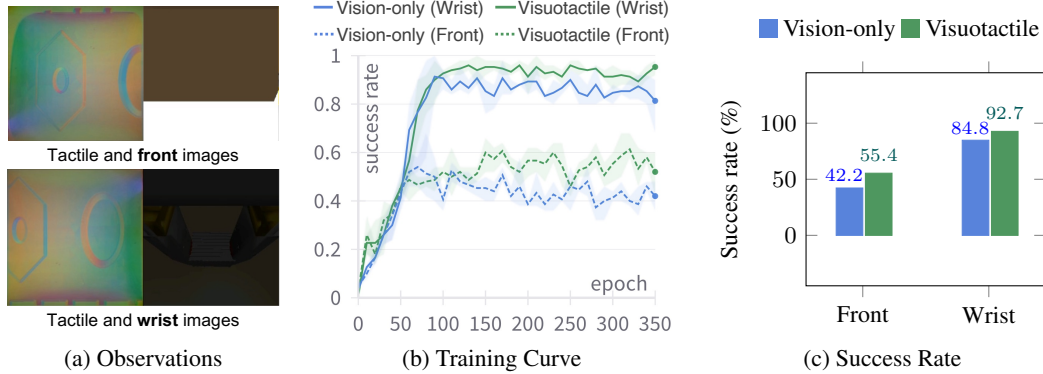


Figure 7: Comparison of front and wrist camera views for vision-only and visuotactile policies in the tactile exploration task. (a) Sample observations showing tactile inputs and visual images from occluded front views and dim wrist views. (b) Training curves comparing policy performance across different viewpoints. (c) Final success rates (%) averaged over the last ten epochs and three seeds.

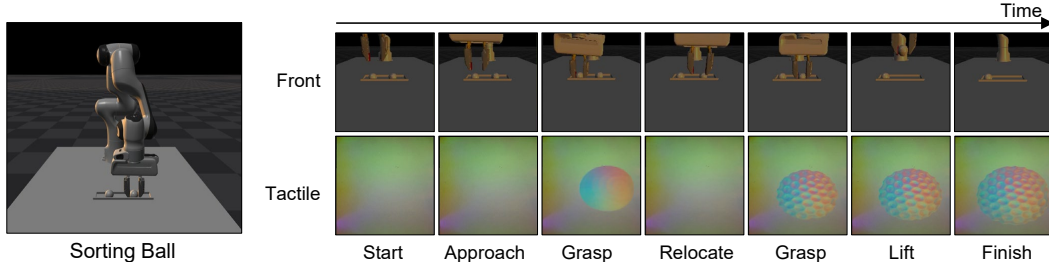


Figure 8: Rollout of the tactile sorting task in the simulation environment under dim lighting conditions. The policy takes front-view and tactile images as multimodal inputs. Note that tactile images are resized to a square shape of 256×256 , from their original resolution of 240×320 .

F.5 Representative Rollouts of Visuotactile Policies

Figs. 8 and 9 visualize policy rollouts for two representative tasks from the ManiFeel benchmark: tactile sorting under dim lighting and blind insertion in a vision-occluded environment. These visualizations show the temporal evolution of observations from multiple sensory channels, including front-facing camera view and tactile inputs, across key action stages. Such rollouts help illustrate how policies leverage tactile feedback when visual inputs are ambiguous or occluded. In the tactile sorting task, for example, tactile observations enable the policy to distinguish between objects with similar visual appearances, such as a table tennis ball and a golf ball, by identifying differences in surface texture. This allows the policy to correct initial grasping errors, such as mistakenly picking up the table tennis ball, by regrasping and successfully retrieving the target golf ball to complete the sorting task. This behavior is particularly valuable under dim lighting conditions, where visual cues alone are insufficient for reliable classification. In the blind insertion task, tactile feedback plays a critical role in implicitly estimating the in-hand pose of the peg, which is otherwise unobservable

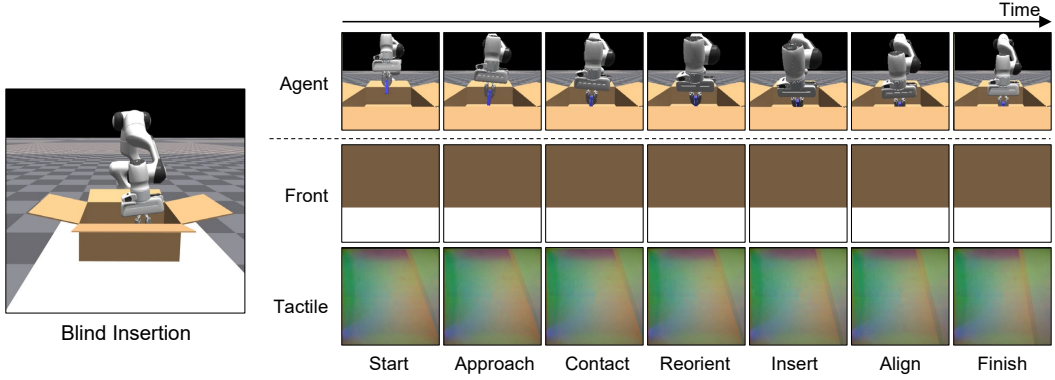
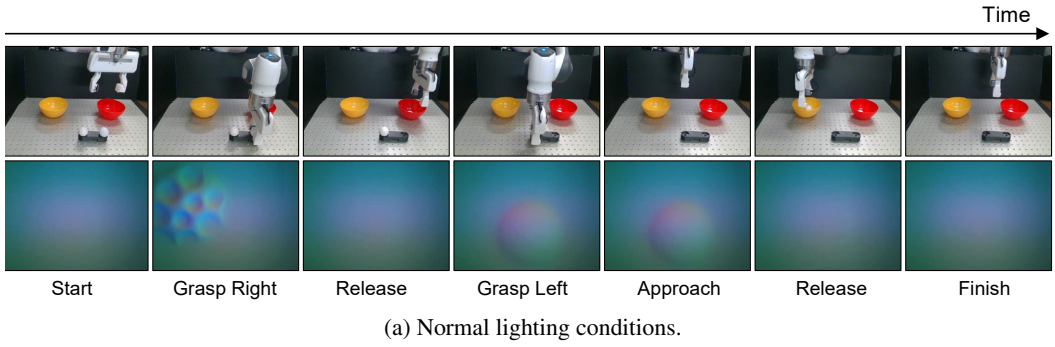
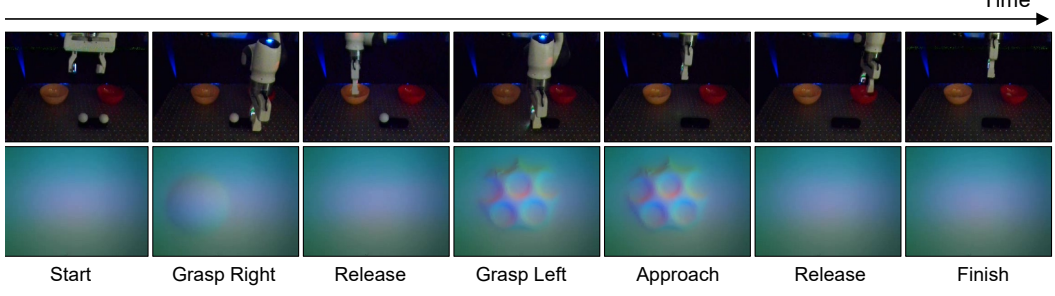


Figure 9: Rollout of the blind insertion task in the simulation environment. The policy takes front-view and tactile images as multimodal inputs. The agent view is shown for visualization purposes only and is not part of the policy’s observation inputs. Note that tactile images are resized to a square shape of 256×256 , from their original resolution of 240×320 .



(a) Normal lighting conditions.



(b) Dim lighting conditions.

Figure 10: Rollouts of the visuotactile policy in the real-world tactile sorting task under (a) normal and (b) dim lighting conditions. The policy receives observations from a front-facing camera and a single left-finger (GelSight) tactile sensor.

due to the occluded visual field inside the closed container. By adapting the grasp and alignment based on contact signals, the policy is able to achieve successful insertions without relying on external visual confirmation. These examples highlight the importance of tactile sensing for robust policy execution in vision-compromised scenarios. Additional examples and full rollouts can be found in the accompanying supplementary video.

F.6 Real-world Experiment

In the real-world experiment, we evaluate the tactile sorting task, where the robot must classify and sort two visually similar spherical objects, a golf ball and a table tennis ball, into designated bowls.

The robot is equipped with a front-facing Intel RealSense camera and a single left-finger tactile sensor (GelSight Mini) for perception. Control is performed using an OSC-yaw controller, which regulates the end-effector’s position and yaw rotation while keeping roll and pitch fixed.

Fig. 10 presents visuotactile policy rollouts under both (a) normal and (b) dim lighting conditions. These visualizations demonstrate how tactile feedback enhances policy robustness, particularly when visual inputs are degraded. For instance, in low-light scenarios, tactile sensing enables the robot to distinguish object surface features and correct initial grasping misalignment. The successful completion of the sorting task under both lighting conditions confirms the value of incorporating tactile perception. Furthermore, the close resemblance between simulated and real tactile feedback, along with consistent policy behavior, highlights the potential of the ManiFeel simulation benchmark and datasets for enabling sim-to-real transfer in visuotactile policy learning. Additional examples and full rollouts can be found in the accompanying supplementary video.